The Large Scale Structure of the Cosmic Microwave Background

E. B. Rørnes*
Institute of Physics, University of Oslo,
0371 Oslo, Norway
(Dated: April 3, 2024)

In this paper we consider the large scale structure of the universe and the Cosmic Microwave Background (CMB) fluctuations...

INTRODUCTION

This project was built on the template provided from [1] which already contains a large part of the structure behind the numerical parts of the project. In the entire paper the subscript 0 denotes today's values... (not a final introduction)

Note that I will fix the font size on the figures to match (or at least be similar) to the text size in the main report as well as move them to more reasonable locations at some later time.

1. MILESTONE I

In this section we consider the evolution of the uniform background of the universe in the ΛCDM (Lambda-Cold-Dark-Matter) model which is considered to be the present day standard model of cosmology. The main goal of this section is to use cosmological parameters to obtain observables and compare observational data.

1.1. Theory

1.1.1. Friedmann-Lemaître-Robertson-Walker

In this milestone we approximate the universe to be completely isotropic and homogeneous over large scales. This has been shown to be a reasonable assumption from observations of the CMB power spectra [2]. With this we arrive at an exact solution for the metric via the Einstein field equations (EFE):

$$G_{\mu\nu} + \Lambda g_{\mu\nu} = 8\pi G T_{\mu\nu}, \tag{1}$$

called the Friedmann-Lemaître-Robertson-Walker (FLRW) metric. In flat space, $k = 0$, and Cartesian coordinates it is given by:

$$g_{\mu\nu} = \text{diag}\left[-c^2, a^2(t), a^2(t), a^2(t)\right],$$

with the mostly plus metric signature $(-,+,+,+)$ and $a(t)$ is the scale factor, defined to be 1 today.

With the FRWL metric and the EFE for a perfect liquid one can derive the Friedmann equations:

$$\left(\frac{\dot{a}}{a}\right)^2 \equiv H^2 = \frac{8\pi G}{3}\rho, \tag{2}$$

$$\frac{\ddot{a}}{a} = -\frac{4\pi G}{3}(\rho + 3p), \tag{3}$$

where ρ and p come from the energy-momentum tensor $T_{\mu\nu}$ for a perfect liquid and is the energy density and pressure respectively of said perfect liquid.

1.1.2. ΛCDM Model

The ΛCDM model is derived by assuming; that we have some family of weakly interacting massive particles (WIMPs) which we call cold-dark-matter (CDM) and that a cosmological constant, Λ, accounts for the acceleration of the universe, which will be the dark energy in this article. The name CDM comes from assuming that they are massive enough to not be relativistic and hence cold.

With these assumptions and approximating that particles behave like perfect fluids, (2) can be rewritten such that the time dependence of the Hubble factor $H \equiv \dot{a}/a$ is given by

$$H^2 = H_0^2 \sum_i \Omega_{i0} a^{-3(1+\omega_i)}$$

where $\omega_i \equiv p_i/\rho_i$ is the equation of state for the i-th particle type, $\Omega_i \equiv \rho_i/\rho_C$ is the relative energy density of the i-th particle type, ρ_i is the energy density corresponding to the i-th particle type and $\sum_i \rho_i = \rho_C$ is the critical energy density required to have a flat universe. We have that $\omega_\text{B} = 0, \omega_\text{R} = 1/3$ and $\omega_\Lambda = -1$ for baryons, relativistic particles (photons and massless neutrinos) and dark energy (DE) respectively. Simply plugging in the various particle types we have:

$$H = H_0\sqrt{\Omega_{\text{M}0}a^{-3} + \Omega_{\text{R}0}a^{-4} + \Omega_{\text{K}0}a^{-2} + \Omega_{\Lambda 0}}, \tag{4}$$
$$\Omega_{\text{M}0} \equiv \Omega_{B0} + \Omega_{\text{CDM}0}, \quad \Omega_{\text{R}0} \equiv \Omega_{\gamma 0} + \Omega_{\nu 0},$$

where Ω_{B0}, $\Omega_{\text{CDM}0}$, $\Omega_{\gamma 0}$, $\Omega_{\nu 0}$ and $\Omega_{\Lambda 0}$ are then the present day relative densities of baryonic matter (electrons & protons), cold dark matter, radiation, neutrinos and dark energy respectively. The term $\Omega_{\text{K}0} = -kc^2/H_0$ denotes the curvature of the universe and encapsulates

* e.b.rornes@fys.uio.no

how said curvature affects expansion rates and energy densities. With the requirement for a flat universe we have that $\sum_i \Omega_i = 1$. Since $\Omega_{\rm B}$, $\Omega_{\rm CDM}$ and Ω_γ, Ω_ν give the same contribution to the time evolution of the Hubble parameter, we will often bundle these together as "matter" and "radiation" (or "relativistic") particles respectively as was done in (4).

The other Friedmann equation (3), together with each particles equation of state, is then used to describe how each component evolves with time:

$$\begin{aligned} \Omega_{\rm B}(a) &= \frac{\Omega_{\rm B0}}{a\mathcal{H}^2/H_0^2}, \quad \Omega_{\rm CDM}(a) = \frac{\Omega_{\rm CDM0}}{a\mathcal{H}^2/H_0^2}, \\ \Omega_\gamma(a) &= \frac{\Omega_{\gamma 0}}{a^2\mathcal{H}^2/H_0^2}, \qquad \Omega_\nu(a) = \frac{\Omega_{\nu 0}}{a^2\mathcal{H}^2/H_0^2}, \\ \Omega_{\rm K}(a) &= \frac{\Omega_{\rm K0}}{\mathcal{H}^2/H_0^2}, \qquad \Omega_\Lambda(a) = \frac{\Omega_{\Lambda 0}}{H^2/H_0^2}, \end{aligned} \tag{5}$$

where $\mathcal{H} \equiv aH$ is the **conformal Hubble factor**. Two of the six density parameters follows from the observed temperature of the CMB and are given by:

$$\Omega_{\gamma 0} = \frac{8\pi^3 G}{45H_0^2}\frac{(k_B T_{\rm CMB0})^4}{\hbar^3 c^5}, \tag{6}$$

$$\Omega_{\nu 0} = \Omega_{\gamma 0} N_{\rm eff} \cdot \frac{7}{8}\left(\frac{4}{11}\right)^{4/3}, \tag{7}$$

where $T_{\rm CMB0}$ is the temperature of CMB photons today and $N_{\rm eff} = 3.046$ is the effective number of massless neutrinos.

The ΛCDM model is then fully determined by these cosmological observables which come from 2018 Planck [3]:

$$\begin{aligned} \frac{H_0\,\mathrm{Mpc}}{100\,\mathrm{km/s}} \equiv h = 0.67, \qquad & N_{\rm eff} = 3.046, \\ \Omega_{\rm B0} = 0.05, \qquad & \Omega_{\rm CDM0} = 0.267, \\ \Omega_{\rm K0} = 0.00, \qquad & T_{\rm CMB0} = 2.7255. \end{aligned} \tag{8}$$

1.1.3. Time and Distance Measurements in Cosmology

Since the universes expansion is strictly positive, the scale factor $a(t)$ is an injective function w.r.t. time and can thus be used as a time measurement. In this paper we will, for computational purposes, be using the variable $x \equiv \ln(a) \implies a = e^x$.

Again, due to the expansion of the universe, one can also measure how much the wavelength of a photon released at initial time t_i has stretched before it reaches us at final time t_f, commonly known as the **redshift**:

$$z = e^{x(t_f)-x(t_i)} - 1.$$

A derivation can be found in [4]. Since we are mainly interested in the redshift w.r.t. today then $x(t_f) = 0$. Thus the formula which will be used in this article is $z = e^{-x(t_i)} - 1$.

Further we consider the **horizon**, i.e. the "distance" massless particles may have travelled since the big bang. Since the universe is expanding, this will be appreciably larger than ct. Considering a time t_1, light would have travelled a distance $d_1 > ct_1$. We can then consider what t_1 must be such that this becomes an equality. For this we define the **conformal time** $d\eta = dt/a$ which can be rewritten as $\eta(t) \equiv \int_0^t \frac{c}{a}dt'$ and we get the differential equation:

$$\frac{d\eta}{dx} = \frac{c}{\mathcal{H}}, \tag{9}$$

along with the initial condition $\eta(-\infty) = 0$, which can be solved analytically in the radiation dominated era. We will then use the analytical solution to approximate that at some very early time, $x_{\rm start}$ such that we have the new initial condition $\eta(x_{\rm start}) = c/\mathcal{H}(x_{\rm start})$ where we will solve onwards numerically.

A useful distance measure is the **comoving distance** χ which is derived by the FLRW metric:

$$\chi = \int_{t_i}^{t_0} dt\frac{c}{a} = \int_1^a da'\frac{c}{a'^2 H} = \int_0^z dz'\frac{c}{H} = \eta - \eta_0.$$

Considering a light-like path with the FLRW metric in curved space one arrives at the **proper distance** r:

$$r = \begin{cases} \chi\frac{\sin(\sqrt{|\Omega_{\rm K0}|}H_0\chi/c)}{\sqrt{|\Omega_{\rm K0}|}H_0\chi/c}, & \Omega_{\rm K0} < 0 \text{ "Closed"} \\ \chi, & \Omega_{\rm K0} = 0 \text{ "Flat"} \\ \chi\frac{\sinh(\sqrt{|\Omega_{\rm K0}|}H_0\chi/c)}{\sqrt{|\Omega_{\rm K0}|}H_0\chi/c}, & \Omega_{\rm K0} > 0 \text{ "Open"} \end{cases}.$$

We then consider the angular **diameter distance** $d_A = \Delta s/\Delta\theta$ where Δs is the objects physical size and $\Delta\theta$ its angular size as viewed from Earth. Once again from the FRLW metric, now in spherical coordinates:

$$ds^2 = -c^2dt^2 + a^2(dr^2 + r^2d\theta^2 + \sin^2\theta d\phi^2),$$

one can find that this can be expressed in terms of our cosmological parameters as $d_A = ar$. The **luminosity distance** d_L is defined from $d_L = \sqrt{\frac{L}{4\pi F}}$ where L is the intrinsic luminosity and F is the measured flux. As implied by its name, this quantity is related to d_A by $d_L = d_A/a^2 = r/a$.

At last we consider the **cosmic time** t in our x coordinate:

$$t(x) = \int_0^a \frac{da}{aH} = \int_{-\infty}^0 \frac{dx}{H(x)}.$$

From this we get to the ODE:

$$\frac{dt}{dx} = \frac{1}{H}, \tag{10}$$

with the initial condition $t(-\infty) = 0$. This initial condition states that cosmic time begins once the big bang happened. As before, we make an analytical approximation which gives us the initial condition $t(x_{\rm start}) = \frac{1}{2H(x_{\rm start})}$ and solved numerically from here.

1.1.4. Markov-Chain Monte Carlo Method

In this milestone one of the major computational method which will be used is the Markov Chain Monte Carlo (MCMC) method. The particular algorithm we use is the Metropolis algorithm which generates a Markov chain, where in each step, the chain corresponds to a proposed set of model parameters, which in our case are h, Ω_{M0} and Ω_{K0}. These parameters are sampled from a probability distribution guided by certain priors, i.e. accepted ranges, where data outside of these priors are omitted . The algorithm then eventually converges to the posterior distribution of the parameters given the observed data. This can then be used to constrain the cosmological parameters, in which we decide to focus on $h, \Omega_{\mathrm{CDM0}}$ and Ω_{M0}. A χ^2-test is then done by the assumption that the measurements are Gaussian distributed and uncorrelated between different redshift. The likelihood function is then given by $L \propto e^{-\chi^2/2}$ where:

$$\chi^2(h, \Omega_{\mathrm{M0}}, \Omega_{\mathrm{K0}}) = \sum_{i=1}^{N} [d_L(z_i, h, \Omega_{\mathrm{M0}}, \Omega_{\mathrm{K0}}) - d_L^{\mathrm{obs}}]^2 / \sigma_i^2.$$

Here σ_i is the standard deviation for the i-th data point and N is the total number of data points. The set of parameters with the highest likelihood is our best-fit model, which also happen to be the values which minimize χ^2. To check that this best-fit is in fact a good fit one can consider a set of data points which all lie exactly 1σ away from the observed values. As such the expression in the sum simply reduces to 1. Thus when summing over N terms equal to 1 we would have that $\chi^2/N = 1$. Hence we will consider a best-fit to be a good fit if $\chi^2 \sim N$. For the case when $\chi^2 \ll N$ then we over-fit the model, meaning we may be capturing random noise and fluctuations in the data, whilst if $\chi^2 \gg N$ then we simply have a bad correspondence with the data and/or underlying assumptions (such as the assumption that the measurements are Gaussian).

Note to self: Add a derivation from Bayes' law and what follows from that.

1.2. Implementation details

1.2.1. Solving the ODEs

To implement some numerical tools to solve for the background we first implement the data from (8) and computed the derived quantities $\Omega_{\gamma 0}$ and $\Omega_{\nu 0}$ with (6,7), and $\Omega_{\Lambda 0} = 1 - \Omega_{\mathrm{rest0}}$ where "rest" refers to all the other Ω_i.

Next we implemented an ordinary differential equation (ODE) solver to solve the ODEs for $\eta(x)$ and $t(x)$. This was done by first setting up the respective differential equation (9,10) with its corresponding initial condition, then an ODE solver was used to get a result which was then splined. The ODE solver and splining programs were already provided in the template.

Further we computed $H(x)$ from (4) which used together with the various relations from the theory section to compute $\mathcal{H}, \frac{d\mathcal{H}}{dx}, \frac{d^2\mathcal{H}}{dx^2}, \Omega_i, r, d_A, d_L, \chi$ and T_{CMB} all as a function of our time variable x. Note that the expressions for $\frac{d\mathcal{H}}{dx}$ and $\frac{d^2\mathcal{H}}{dx^2}$ were found analytically. The calculated data was then written to data files to be analyzed in Python.

1.2.2. MCMC fit

We then compared our numerical data for the luminosity distance d_L to observational data from [5], containing $N = 31$ data points, by performing an MCMC fit. The upper and lower priors which were used are $\{1.5, 1, 1\}$ and $\{0.5, 0, -1\}$ for h, Ω_{M} and Ω_{K} respectively. The algorithm then computes an initial χ^2 with some randomly generated parameters. It repeats this process and checks whether the new χ^2_{new} is less than the old χ^2_{old}, if this is the case then it accepts this sample and starts again. However if this previous test is not the case we then perform a random check $e^{-(\chi^2_{\mathrm{new}} - \chi^2_{\mathrm{old}})/2} > u$ where u is number drawn from a uniform distribution in the interval $[0, 1]$. If it passes this test then χ^2_{new} is accepted and the process carries on. This additional test is the main part of the Metropolis algorithm and is done to capture the full posterior probability distribution function (PDF) of the various parameters. As before, the data was printed to a data file and imported to Python.

1.2.3. Python

x-values corresponding to radiation-matter- and matter-DE-equality were found by finding running a script over the data to find where the absolute value of the difference $|\Omega_i - \Omega_j| = 0$. In reality they were never quite 0 due to running over a discrete index, thus we simply set some low threshold, e.g. $5 \cdot 10^{-5}$. To find when the universe accelerates we note that:

$$\mathcal{H} = \frac{\dot{a}}{a} a = \dot{a} \implies \frac{d\mathcal{H}}{dx} = \frac{d\mathcal{H}}{dt}\frac{dt}{dx} = \ddot{a}\frac{dt}{dx},$$

and from (10) we then have:

$$\frac{d\mathcal{H}}{dx} \equiv \mathcal{H}' = \frac{\ddot{a}}{H}.$$

Since H is strictly positive we can then look at when $\mathcal{H}'$ changes from negative to positive. So again a Python script which runs over the indices of $\mathcal{H}$ were used to find which x-values this sign change happened, which corresponds to where the universe began to accelerate.

The MCMC-fit was then analyzed and a scatterplot in the $\Omega_\Lambda \Omega_{\mathrm{M}}$-plane was created with the $(1\sigma, 2\sigma)$ confidence

regions $\chi^2 - \chi^2_{\min} < (3.53, 8.02)$ respectively. These particular values were found from common χ^2 distribution tables with $k = 3$ degrees of freedom. A histogram of the PDF from the accepted samples of h along with a Gaussian fit was along with a comparison of our theoretical d_L vs. the real supernova data were also plotted.

1.3. Tests of data

Before considering the results it is reasonable to conduct some sanity checks on the data. We first consider Ω_i as given in FIG. 1. Here we can clearly see the different regimes of the various quantities. To check that the data is consistent with the analytical expressions we consider the following quantities analytically in the different regimes:

FIG. 1. Time evolution of the density parameters Ω_i as a function of the scale factor a.

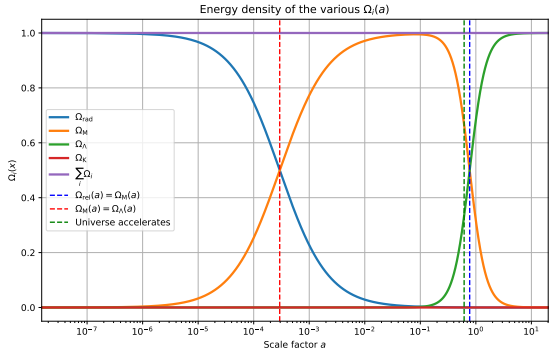

$$\frac{\mathcal{H}'}{\mathcal{H}}, \qquad \frac{1}{\mathcal{H}}\frac{d^2\mathcal{H}}{dx^2} \equiv \frac{\mathcal{H}''}{\mathcal{H}}, \qquad \frac{1}{c}\eta\mathcal{H}.$$

1.3.1. $\mathcal{H}'$ and $\mathcal{H}''$

In the radiation dominated era where we approximate $\Omega_R \approx 1 \implies \Omega_{rest} \approx 0$. Then by using (4) we find:

$$H_R(x) \approx H_0, \quad \mathcal{H}_R(x) \approx H_0 e^{-x},$$
$$\frac{\mathcal{H}'_R}{\mathcal{H}_R} \approx -1, \qquad \frac{\mathcal{H}''_R}{\mathcal{H}_R} \approx 1,$$

and similarly using the approximations $\Omega_M \approx 1$ and $\Omega_\Lambda \approx 1$ respectively, we get:

$$H_M(x) \approx H_0 e^{x/2}, \quad \mathcal{H}_M(x) \approx H_0 e^{-x/2},$$
$$\frac{\mathcal{H}'_M}{\mathcal{H}_M} \approx -1/2, \qquad \frac{\mathcal{H}''_M}{\mathcal{H}_M} \approx 1/4,$$
$$H_\Lambda(x) \approx H_0, \qquad \mathcal{H}_\Lambda(x) \approx H_0 e^{x},$$
$$\frac{\mathcal{H}'_\Lambda}{\mathcal{H}_\Lambda} \approx \frac{\mathcal{H}''_\Lambda}{\mathcal{H}_\Lambda} \approx 1.$$

Plotting these assumptions with the data we have FIG. 2. We see that there is a reasonable agreement with the analytical approximations in the given regimes. As can be seen from FIG. 1, $\Omega_M \approx 1$ is a relatively poor approximation compared to the others, hence larger a deviation is to be expected.

FIG. 2. $\mathcal{H}'/\mathcal{H}$ and $\mathcal{H}''/\mathcal{H}$ compared to analytical approximations.

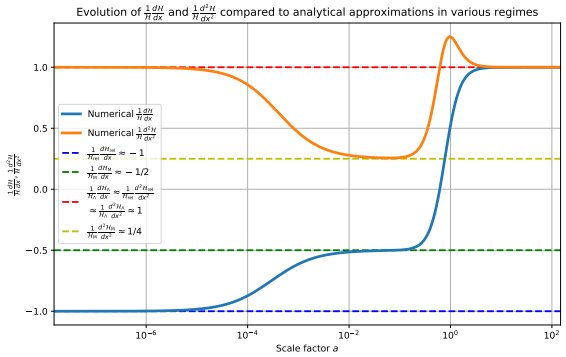

1.3.2. Conformal Time

Analytical approximations for the conformal time requires a little more effort. For the radiation dominated era we can solve (9) analytically:

$$\eta_R(x) = \int_{-\infty}^{x} \frac{c}{\mathcal{H}_R} dx' \approx \int_{-\infty}^{x} \frac{c}{H_0} e^{x'} dx' = \frac{c}{H_0} e^x.$$

Now we approximate this radiation dominated epoch to end abruptly at some time x_1 such that we can write the conformal time in the matter dominated epoch as:

$$\begin{aligned}\eta_M(x) &\approx \eta_R(x_1) + \int_{x_1}^{x} \frac{c}{\mathcal{H}_M} dx' \\ &\approx \frac{c}{H_0}\left(e^{x_1} + \int_{x_1}^{x} e^{x'/2} dx'\right) \\ &= \frac{c}{H_0}(e^{x_1} - 2e^{x_1/2} + 2e^{x/2}).\end{aligned}$$

Again we assume that the matter dominated epoch ends abruptly at some time x_2 such that we can approximate:

$$\begin{aligned}\eta_\Lambda(x) &\approx \eta_M(x_2) + \int_{x_2}^{\infty} \frac{c}{\mathcal{H}_\Lambda} dx' \\ &\approx \frac{c}{H_0}\left(e^{x_1} - 2e^{x_1/2} + 2e^{x_1/2} + \int_{x_2}^{x} e^{-x'} dx'\right) \\ &= \frac{c}{H_0}\left(e^{x_1} - 2e^{x_1/2} + 2e^{x_2/2} + e^{-x_2} - e^{-x}\right).\end{aligned}$$

Thus we find that for the various regimes we have:

$$\eta_{\mathrm{R}}\mathcal{H}_{\mathrm{R}}/c \approx 1,$$
$$\eta_{\mathrm{M}}\mathcal{H}_{\mathrm{M}}/c \approx (e^{x_1} - 2e^{x_2/2} + 2e^{x/2})e^{-x/2},$$
$$\eta_{\Lambda}\mathcal{H}_{\Lambda}/c \approx (e^{x_1} - 2e^{x_1/2} + 2e^{x_2/2} + e^{-x_2} - e^{-x})e^{x}.$$

Using the x values corresponding to $\Omega_{\mathrm{R}} = \Omega_{\mathrm{M}}$ and $\Omega_{\mathrm{M}} = \Omega_{\Lambda}$ as the time where the respective epochs start and end we get the upper graph in FIG. 3. Clearly this approximation will be nothing close to exact due to the assumption that the epochs end abruptly when in reality the epoch's change continuously and relatively slowly. Since η depends on how long the previous epochs lasted we can see that this heavily affects the final epoch. Remove: If we instead rather arbitrarily consider each epoch to end where the respective density parameters fall below 85% then we have a plot which suits the data much better which is the lower graph in FIG. 3.

FIG. 3. Numerical $\eta\mathcal{H}/c$ compared to analytical approximations in the various regimes where epochs are approximated to abruptly once $|\Omega_i - \Omega_j| = 0$ and $\Omega_i < 0.85$ respectively.

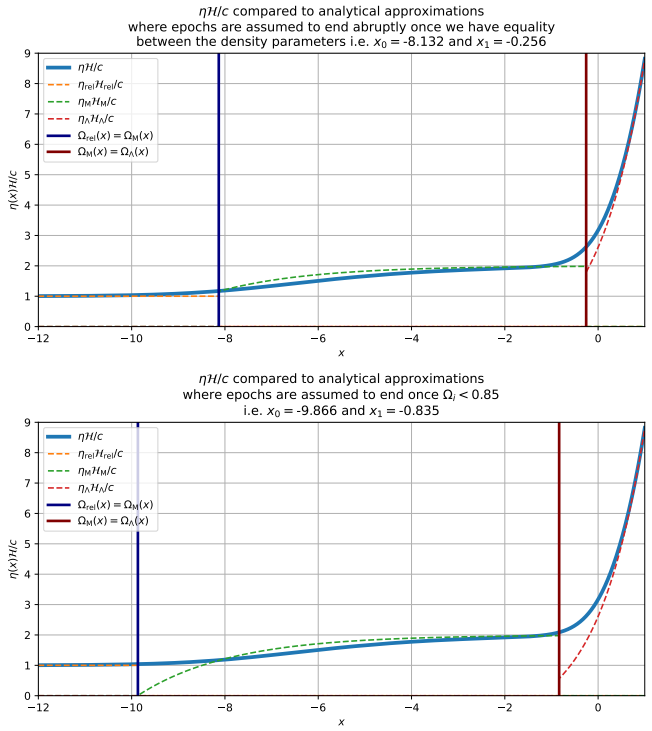

Overall the data seems to be consistent with the analytical expressions, even if the conformal time is a rather difficult parameter to define a robust approximation for.

1.4. Results

Now that the data has been stress tested to show that they are at least valid in certain regions we can go on to look at some of the results.

1.4.1. Time Evolution of Cosmic Parameters

The time evolution of the conformal Hubble factor $\mathcal{H}(x)$, cosmic time $t(x)$ and conformal distance $\eta(x)/c$ is given in FIG. 4. The notable acceleration at later times in the $\mathcal{H}$ plot can be seen by when the derivative of $\mathcal{H}$ changes sign as mentioned previously. One can also see that this same phenomena affects both the cosmic time and conformal distance inversely at the same time. This is due to them both being inversely proportional to the conformal Hubble factor.

FIG. 4. Time evolution of the conformal Hubble factor $\mathcal{H}$, cosmic time t and conformal distance η/c as a function of x.

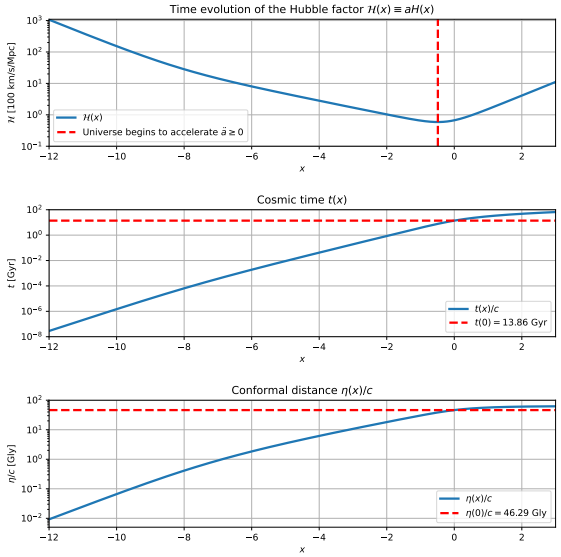

Next we consider the values of $x, z, t, \eta, \Omega_{\mathrm{M}}, \Omega_{\Lambda}$ and Ω_{R} at various important events. A summary of these events is given in TABLE I.

Here we can see that radiation-matter-equality happened roughly 51000 years after the big bang. This is a similar value to other reported figures cite (x,y,z). Further, the universe begins to accelerate roughly 7.7 billion years after the big bang. One may notice that this happens $2\Omega_{\Lambda} \approx \Omega_{\mathrm{M}}$ and $\Omega_{\mathrm{others}} \approx 0$. We can check this analytically by considering these approximation. We have that $\Omega_{\mathrm{tot}} \approx 3\Omega_{\Lambda}$ and hence $\rho_{\mathrm{tot}} = 3\rho_{\Lambda}$. Further we have that $p_{\mathrm{tot}} = p_{\Lambda} + p_{\mathrm{M}} = p_{\Lambda}$ due to $p_{\mathrm{M}} = 0$ from its equation of state. Inserting this into the Friedman equation (3) with the relevant equation of state we get:

$$\frac{\ddot{a}}{a} \approx -\frac{4\pi G}{3}(3\rho_{\Lambda} + 3(p_{\Lambda} + p_{\mathrm{M}}))$$
$$= -\frac{4\pi G}{3}(3\rho_{\Lambda} - 3\rho_{\Lambda}) = 0$$

TABLE I. Results for cosmological parameters at various important events from numerical data.

Event	x	$z(x)$	$t(x)$ [Gly]	$\eta(x)/c$ [Gly]	Ω_{M}	Ω_{Λ}	Ω_{Rel}
Radiation-Matter Equality	-8.132	3401	$5.106 \cdot 10^{-5}$	0.368	0.500	$2.737 \cdot 10^{-11}$	0.500
Universe Accelerates	-0.486	0.626	7.761	38.55	0.666	0.334	$3.183 \cdot 10^{-4}$
Matter-DE Equality	-0.256	0.292	10.38	42.33	0.500	0.500	$1.900 \cdot 10^{-4}$
Universe Today	0.000	0.000	13.86	46.29	0.317	0.683	$9.320 \cdot 10^{-5}$

Now, since a is strictly a positive number then, mathematically, all that remains to check whether this is not when deceleration starts or some top point. To ensure this one can just check some arbitrarily close points such as $\Omega_{\Lambda} = 1/3 \pm \epsilon$ and $\Omega_{\mathrm{M}} = 2/3 \mp \epsilon$ where ϵ is some tiny positive number. Maybe show this explicitly at some later time.

Next in the table we have $t(x = 0)$ which corresponds to the age of the universe today. [**?**] estimates this to be $13.78 \pm 0.20\,\mathrm{Gly}$ (Giga light years) which is reasonably close to our value of 13.86 Gly. Similarly $\eta(x = 0)$ shows us the actual size of the observable universe today. Various sources (x,y,z) show that the expected conformal distance of the universe should be slightly above 46 Glyr, once again in agreement with the data.

1.4.2. Supernova Comparison

Further we compare our numerical data to data collected from supernova observations [5, Betoule et al. 2014] by; comparing the luminosity distance is given in FIG. 5 and making a PDF of the Hubble parameter H_0 in FIG. 6. We note that the found $\chi^2_{\mathrm{min}} = 29.3$ for the MCMC fit, which then yields that for the points accepted within the 1σ region follow $\chi^2 \sim N$ to a very good approximation, suggesting that we have a good fit.

The luminosity distance from observational data is seemingly always lower than our data. This phenomena is known as the **Hubble tension** which is a widely known problem in today's standard model of cosmology [6]. Direct data, such as supernova data, seemingly always prefers lower values for luminosity distance, and thus, higher values for h that can be seen in FIG. 6. Indirect data, such as the CMB, however prefer higher values for d_L and thus lower values h with much smaller errorbars. This is an ongoing issue which suggests that the ΛCDM model is not a complete model and must be modified. The posterior PDF of the Hubble parameter today H_0 shows that the Gaussian fit is centered at roughly 70.1 km/s/Mpc. As mentioned, this is a large discrepancy from $H_0 = 67\,\mathrm{km/s/Mpc}$ which we got from the fiducial cosmology but still considered a common result from direct data.

Next we consider the scatterplot in the $\Omega_{\Lambda}\Omega_{\mathrm{M}}$-plane shown in FIG. 7. The scatter-plot helps us visualize the degeneracy between the density parameters, i.e. that many different combinations of Ω_{M} and Ω_{Λ} can yield similar observational results. This leads to rather large

FIG. 5. Luminosity distance over redshift z, plotted against redshift z for both; our numerical data, and observational data from Betoule [5] with error-bars.

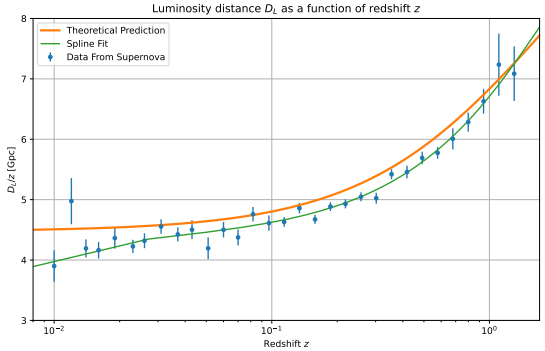

FIG. 6. Posterior PDF of the Hubble parameter H_0.

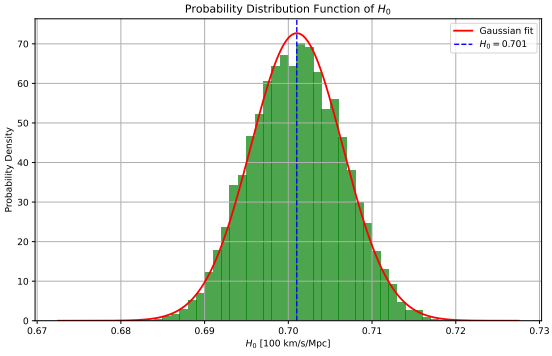

degenerate regions in the parameter space. In this figure we can see that the flat universe constraint significantly reduces this degeneracy by lowering the allowed parameters by multiple orders of magnitude. The figure clearly shows that $\Omega_{\Lambda 0} = 0$ is completely excluded given the observational data as this would be far outside the 2σ constraint. The best-fit value for $\Omega_{\mathrm{K}0} = 0.067$ tells us that the universe is seemingly quite flat, but that there is indeed some curvature. To test out whether this might just be an insensitivity to the $\Omega_{\mathrm{K}0}$ parameter the code was run again with a large initial value $\Omega_{\mathrm{K}0}$. The result did not seem to change whatsoever and thus this...

FIG. 7. Supernova data with 1σ and 2σ constraints from MCMC fits.

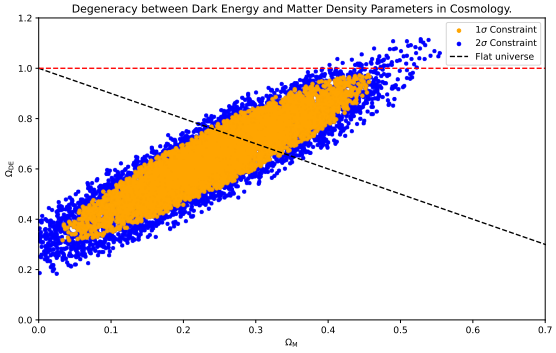

1.5. Summary & Conclusion

To summarize, we numerically solved the ODEs for η and t past the radiation domination. We then computed $H(x)$ which gave us access to all the other relevant cosmological parameters. We then performed an MCMC fit with observational data from supernova events and the numerical data. Further we checked that the numerical data corresponds to analytical approximations in the different regimes. Next we introduced all the most relevant data in a graphed form in FIG 4-6 such that important events and values were easily visualized. Finally the most relevant values were summarized in TABLE I.

In conclusion, the data all seems to correspond quite well with observational data and previous calculations from more sophisticated methods.

2. MILESTONE II

Next we look at the recombination history of the universe. This is when baryons, mainly protons and electrons, went from being ionized to forming neutral atoms once the energy of the photons dropped below 13.6 eV. As a result, photons during this time decoupled from the thermal equilibrium of the universe and are what we now detect as the CMB photons. As this event is tightly related to the free mean path of photons, the goal of this section is to compute the optical depth τ, the visibility function $\tilde{g}$ and their derivatives. In this project we only consider the formation of hydrogen and neglect the existence of any heavier atoms.

To accomplish this we start by calculating the free electron fraction X_e which we will first compute from the Saha equation in early times till $X_e < 0.99$ and then switch over to Peebles' equation from thereon. The reason we don't use Peebles' equation from the start is due to it being extremely sensitive to high temperatures and thus the solution at early times is very unstable.

2.1. Theory

As eluded to in the intro we will consider the optical depth $\tau(x)$ which is defined by the relation:

$$I(r) = I_0 e^{-\tau(r)}, \tag{11}$$

where I_0 is the intensity of a source which emits radiation and $I(r)$ is the intensity that an observer at a distance r would detect. Here we can clearly see that if $\tau = 0$ then $I(r) = I_0$ and thus the medium the radiation travels through does not affect the intensity. If $\tau \gg 1$ then we say that the medium is optically thick and $\tau \sim 1$ is the transition between the two.

In cosmology the main effect contributing to the optical depth is Thompson scattering of photons with free electrons. A more convenient form for the optical depth in the context of this text is:

$$\tau(\eta) = \int_{\eta}^{\eta_0} d\eta' \, n_e \sigma_T a, \tag{12}$$

where n_e is the number density of free electrons and $\sigma_T = \frac{8\pi}{3}\frac{\alpha^2\hbar^2}{m_e^2c^2}$ is the Thompson cross section which is found from QFT calculations. (12) can be rewritten into differential form:

$$\frac{d\tau}{dx} = -\frac{cn_e\sigma_T}{H}, \tag{13}$$

which is the ODE that we will solve. Since we see that the optical depth today is 0 we have the initial condition $\tau(0) = 0$. On the RHS of (13) the only missing factor is n_e. Instead of computing n_e directly we will consider the fractional electron density:

$$X_e \equiv n_e/n_H \approx \frac{n_e m_H}{\rho_b} = \frac{n_e m_H a^3}{\Omega_{\mathrm{B0}}\rho_{c0}},$$

where the approximation is due to us not considering any heavier elements than hydrogen. To do this we consider the Saha equation:

$$\frac{n_e n_p}{n_e^{(0)} n_p^{(0)}} = \frac{n_H n_\gamma}{n_H^{(0)} n_\gamma^{(0)}},$$

Here n_p, n_γ and n_H are the number densities for free protons, photons and Hydrogen atoms respectively and (0) represents that the given number density is in the thermal equilibrium. This is an analytical approximation for when the interaction rate is very high compared to the change in electron density. Since in the early universe consists purely of free electrons due to the high temperatures of the primordial plasma, this then suggests that the Saha equation is only valid when $X_e \approx 1$. Given our definition of X_e and the approximations we can rewrite the Saha equation to the convenient form:

$$\frac{X_e^2}{1 - X_e} = \frac{1}{n_b}\left(\frac{k_b m_e T_b}{2\pi\hbar^2}\right)^{3/2} e^{-\epsilon_0/k_b T_b}, \tag{14}$$

where T_b is the baryon temperature of the universe and $\epsilon_0 = 13.6\,\text{eV}$ is the ionization energy of hydrogen. In reality there should also be a T_γ in this equation representing the temperature of photons at a given time, but in practice it is an excellent approximation to set $T_\gamma = T_b = T_{\text{CMB0}}/a$. The rewritten Saha equation is now simply a 2nd order polynomial in X_e which is easily solved analytically:

$$X_e = \frac{C}{2}\left[\sqrt{1+\frac{4}{C}} - 1\right], \tag{15}$$

$$C \equiv \frac{1}{n_b}\left(\frac{k_b m_e T_b}{2\pi\hbar^2}\right)^{3/2} e^{-\epsilon_0/k_b T_b}, \tag{16}$$

where we have omitted the negative solution due to the electron fraction being manifestly positive. We also note that in the limit $4/C \ll 1$ then $X_e = 1$ which will be used in the numerical part later.

Since the Saha equation is only valid for $X_e \approx 1$ then, as noted earlier, we consider Peebles' equation outside this realm. The derivation for Peebles' equation is beyond the scope of this paper and can be found at (cite x) and is given by:

$$\frac{dX_e}{dx} = \frac{C_r(T_b)}{H}\left[\beta(T_b)(1-X_e) - n_H X_e^2 \alpha^{(2)}(T_b)\right], \tag{17}$$

where

$$\begin{aligned}
C_r(T_b) &= \frac{\Lambda_{2s\to 1s} + \Lambda_\alpha}{\Lambda_{2s\to 1s} + \Lambda_\alpha + \beta^{(2)}(T_b)},\\
\Lambda_{2s\to 1s} &= 8.227\,\text{s}^{-1},\\
\Lambda_\alpha &= H\frac{(3\epsilon_0)^3}{(8\pi)^2 c^3 \hbar^3 n_{1s}},\\
n_{1s} &= (1-X_e)n_H,\\
n_H &= n_b,\ \text{(no helium)}\ (*)\\
n_b &= \frac{3H_0^2\Omega_{b0}}{8\pi G m_H a^3},\\
\beta^{(2)}(T_b) &= \beta(T_b)e^{\frac{3\epsilon_0}{4k_bT_b}},\\
\beta(T_b) &= \alpha^{(2)}(T_b)\left(\frac{m_e k_b T_b}{2\pi\hbar^2}\right)^{3/2} e^{-\frac{\epsilon_0}{k_b T_b}},\\
\alpha^{(2)}(T_b) &= \frac{8}{\sqrt{3\pi}} c\sigma_T \sqrt{\frac{\epsilon_0}{k_b T_b}}\phi_2(T_b),\\
\phi_2(T_b) &= 0.448\ln\left(\frac{\epsilon_0}{k_b T_b}\right).
\end{aligned}$$

(∗) Shouldn't $n_H = n_b/2$ if we include electrons into our definition of baryons with the assumptions that there are equally many protons as electrons? Or are we suddenly switching over to the particle physics definition of baryons? This ODE will then be solved numerically to find $X_e(x)$ with the initial condition given from the last X_e value from the Saha solution. This then gives us $n_e(x)$ from the definition of X_e which will then be used to solve (13) for $\tau(x)$.

Further we consider the visibility function:

$$\tilde{g}(x) \equiv \frac{d}{dx}e^{-\tau(x)} = -e^{-\tau(x)}\tau'(x), \tag{18}$$

which describes the probability density for a given photon to having its final scattering at time x. Since this is a probability density then it must satisfy

$$\int_{-\infty}^{0} dx\,\tilde{g}(x) = 1$$

The visibility function can be thought of as the probability that a photon scattering between time x and $x+dx$ is the last time it ever scatters before it moves freely. From this we can then consider **last scattering** to occur when the visibility function peaks. The solution to $\tau(x)$ and its derivative makes getting the visibility function a trivial task.

Finally we have the sound-horizon $s(x)$ which is given by:

$$s(x) \equiv \int_0^a dt\,\frac{c_s}{a}, \tag{19}$$

where $c_s = c\sqrt{\frac{R}{3(1+R)}}$ is the sound-speed of the coupled photon-baryon plasma and $R = \frac{4\Omega_{\gamma 0}}{3a\Omega_{\text{B0}}}$. We can rewrite (19) into a differential form as such:

$$\frac{ds}{dx} = \frac{c_s}{\mathcal{H}}, \tag{20}$$

with the initial condition $s(x_{\text{ini}}) = \frac{c_s(x_{\text{ini}})}{\mathcal{H}(x_{\text{ini}})}$.

2.2. Implementation details

2.2.1. Solving the Saha and Peebles' equation

We began by implementing a for-loop for the Saha equation which at each iteration checks whether we are still in the Saha regime. Note that we have to be careful about round-off errors when solving the Saha equation when the term ϵ_0/k_bT_b in the exponential in (16) goes to very small values the rest of the expression will begin to explode. Thus in (15) we would be subtracting two very large numbers which should at the end simplify to just 1 leading to potential round-off errors. To avoid this we instead performed an `if`-test to check whether $4/C$ is less than some small threshold. Once this is the case then we simply set X_e to 1. A justification for this can be seen by considering the first order expansion of the square root in (15), which will just yield $X_e = 1$. Since the Saha equation is only valid for $X_e \approx 1$ we decide to switch over to the more accurate Peebles' equation $X_e < 0.99$. For reference we continued on with the Saha equation past its validity to compare the results.

Peebles' equation was then solved numerically via the same ODE solver used in the previous milestone with

the initial condition supplied by the last point before we exited the Saha regime. Some care was taken to ensure no overflow due to the exponential in the $\beta^{(2)}$ equation under (17). To do this we simply created another `if`-test to check when the term in the exponential exceeded 150 and set $\beta^{(2)} = 0$ as the exponential from β will dominate over it. We then had the results for X_e which we used to compute n_e for both cases. The results for both the Saha only and the Saha-Peebles computations were splined and printed to a data file.

2.2.2. *Solving for the optical depth and visibility functions*

Next we solved the ODE for both the optical depth $\tau(x)$ in eq. 13 and the sound-horizon $s(x)$ with the before mentioned initial conditions. Note that the prior ODE, if computed it in the usual way, one would need to subtract an initial condition off the solution for $\tau(x = 0)$ which would lead to round-off errors close to $x = 0$ due to the finite precision of floating point numbers. This would then lead to noise in the solution and thus the ODE was then instead solved by going backwards in time to avoid this problem. After, $\tau'(x)$ was also computed since the spliner we are working with seemingly does not work well past 1st derivatives since we also want to look at $\tau''(x)$. With both $\tau(x)$ and $\tau'(x)$ we could easily calculate the visibility function $\tilde{g}(x)$ with (18) and its first derivative. These were then all splined along with using the `deriv_x` function in the spliner s.t. we have access to the 2nd derivatives. All the data was again printed to the aforementioned data file.

With the various splines we then calculated the time at recombination and last scattering. Our definition for when recombination happens is when X_e drops below 0.1. We have 2 different definitions for when last scattering occurred; when $\tilde{g}$ peaks and when $\tau = 1$. This was done by iterating through the data in `C++` until these conditions were met.

2.2.3. *Python*

As before the data was imported to Python and various plots together with a table of the various events were made.

2.3. Results

2.3.1. *Recombination Events*

We first consider the quantities x, z, y and r_s at both recombination and when last scattering occurred. The results are summarized in TABLE II where "w/ τ" refers to the definition of last scattering where $\tau = 1$. This seems to give the result that last scattering happened before recombination. This is of course unreasonable as recombination causes last scattering to occur, thus for future reference the peak of $\tilde{g}$ will be chosen as our definition for last scattering. [I don't entirely see the point in even considering $\tau = 1$ as the definition as its quite arbitrary. I sort of want to create some argument for why to exclude it as it does not make much sense regarding the theory. In the end I find that I really just want to exclude any mention of it entirely but since it was mentioned in the milestone text I figured that we are expected to comment on it.] The times for recombination and last scattering both are in agreement previously found values (cite x,y,z).

TABLE II. Recombination Events

Event	x	z	t [kyr]	r_s [Mpc]
Recombination	-6.9855	1079.8	377.96	145.278
Last scattering	-6.9853	1079.7	378.04	145.292
Last scattering w/ τ	-6.9878	1082.3	376.51	145.062

2.3.2. *Electron Fraction X_e*

The results for the electron fraction X_e are given in FIG. 8. Here we see that the moment the electron fraction deviates even a small amount from $X_e = 1$ then the Saha equation plummets, suggesting that recombination would happen at some time $x \sim -7.14$ instead of the value given in TABLE II with Peebles' more accurate equation. In this figure, freeze out refers to the present day abundance of free electron which we find to be $X_e(0) \approx 2.03 \cdot 10^{-4}$.

FIG. 8. Time evolution of the free electron fraction $X_e(x)$.

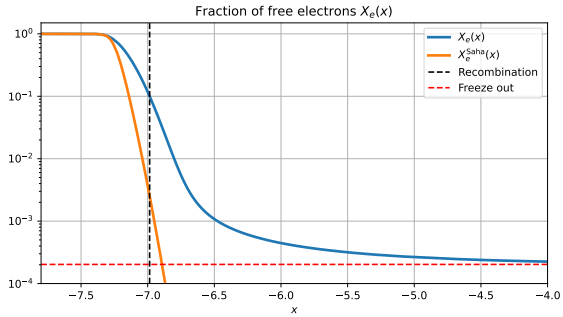

2.3.3. *Evolution of Optical Depth and Visibility function*

Further we consider the time evolution of the optical depth parameter, the visibility function and their derivatives given in FIG. 9 and 10 respectively. The negative of the first derivative of τ is plotted s.t. we can read off all of them in a single log-plot and for a similar reason

the derivatives of $\tilde{g}$ are normalized such that their peak is at $\max \tilde{g}$. The surface of last scattering with the $\tilde{g}$ peak definition is shown for reference.

FIG. 9. Time evolution of the optical depth $\tau(x)$ and its derivatives.

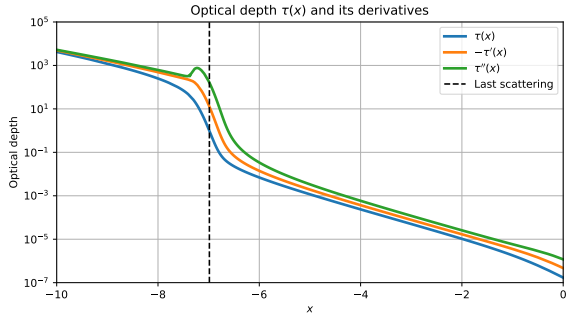

FIG. 10. Time evolution of visibility function $\tilde{g}$ and its derivatives all normalized s.t. $\max|\tilde{g}| = \max|\tilde{g}'| = \max|\tilde{g}''|$ So that it all fits in the same plot. These scale factors are roughly 10 and 200 for $\tilde{g}'$ and $\tilde{g}''$ respectively.

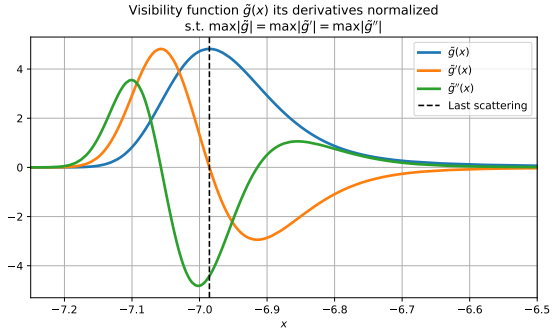

Before this dashed line signaling the last scattering event, the primordial plasma is optically thick, thus the mean free path of photons is too short and will continue on scattering. However, the optical depth at this time still endures a stable decay almost solely due to the expansion rate of the universe as this causes the number density n_e to decrease. This relation can be seen in (12). As mentioned previously, the visibility function is the probability density that a given photon had its last scattering at time x. Thus we can see that when the optical depth is very high, the likelihood of a particular photon at that time scattering for the last time is very small.

$\tau(x)$ then dips down violently as the number of free electrons in the universe rapidly decays. At the same time we then see that this is when the visibility function begins to rapidly increase. This clearly shows that the formation of neutral Hydrogen happens much faster than the expansion of the universe, hence having the largest effect in this epoch. This in turn means that the mean free paths of photons increase beyond the horizon and thus, photons are effectively free to travel without interacting with matter. This is then the last scattering event and the photons released here are the ones that we detect today in the CMB spectra.

Once the electron fraction begins to flatten out again, the optical depth becomes a straight line on the log-plot, once again caused by the expansion of the universe. The visibility function also begins to flatten out at this point, albeit at a slower rate than the initial increase before last scattering.

2.4. Conclusion

We can readily note from FIG. 10 that recombination and last scattering did not happen instantaneously, as $\tilde{g}(x)$ would take the form of a Dirac-delta function, but instead over a relatively short period of time. Due to the short time frame, the number of free electrons in the universe rapidly decreased over several orders of magnitude. The values in TABLE II show us that recombination generally happens first, with the last scattering following shortly after.

As expected from the assumptions made in the derivation of the Saha equation, we see that it quickly becomes a terrible approximation outside of its regime. The manifestly seen correlation between the change in fraction of free electrons, optical depth and the visibility function is also clearly seen, but is of no surprise from their various relations.

3. MILESTONE III

Some introduction about what it is all about.

3.1. Theory

The theory behind this milestone.

3.2. Implementation details

Something about the numerical work.

3.3. Results

Show and discuss the results.

4. MILESTONE IV

Some introduction about what it is all about.

4.1. Theory

The theory behind this milestone.

4.2. Implementation details

Something about the numerical work.

4.3. Results

Show and discuss the results.

ACKNOWLEDGMENTS

...

[1] H. A. Winther, H. K. Eriksen, O. Elgaroy, D. F. Mota, and H. Ihle, "Cosmology ii." `https://cmb.wintherscoming.no/`, 2023. Accessed on March 1, 2023.

[2] S. Dodelson, *Modern Cosmology*. Academic Press, Amsterdam, 2003.

[3] Planck: N. Aghanim *et. al.*, *Planck 2018 results. VI. Cosmological parameters*, *Astron. Astrophys.* **641** (2020) A6, [`arXiv:1807.06209`]. [Erratum: Astron.Astrophys. 652, C4 (2021)].

[4] T. M. Davis and C. H. Lineweaver, *Expanding confusion: Common misconceptions of cosmological horizons and the superluminal expansion of the universe*, *Publications of the Astronomical Society of Australia* **21** (2004) 97–109.

[5] SDSS: M. Betoule *et. al.*, *Improved cosmological constraints from a joint analysis of the SDSS-II and SNLS supernova samples*, *Astron. Astrophys.* **568** (2014) A22, [`arXiv:1401.4064`].

[6] E. Di Valentino, O. Mena, *et. al.*, *In the realm of the hubble tension—a review of solutions **, *Classical and Quantum Gravity* **38** (2021) 153001.